Tetrahedron xxx (2017) 1–10

Contents lists available at ScienceDirect

Tetrahedron

journal homepage: www.elsevier.com/locate/tet

A fluorescent chemosensor for relay recognition of Fe^{3+} and PO_4^{3-} in aqueous solution and its applications

Renjie Liu [a], Xu Tang [a], Yun Wang [a, **], Juan Han [b], Huiqin Zhang [c], Chen Li [a], Wenli Zhang [a, *], Liang Ni [a], Haoran Li [d]

[a] School of Chemistry and Chemical Engineering, Jiangsu University, Zhenjiang, 212013, PR China
[b] School of Food and Biological Engineering, Jiangsu University, Zhenjiang, 212013, PR China
[c] Zhenjiang Entry-exit Inspection Quarantine Bureau, State Key Laboratory of Food Additive and Condiment Testing, Zhenjiang, Jiangsu Province, 212013, China
[d] Department of Chemistry, ZJU-NHU United R&D Center, Zhejiang University, Hangzhou, 310027, PR China

ARTICLE INFO

Article history:
Received 4 May 2017
Received in revised form
10 July 2017
Accepted 11 July 2017
Available online xxx

Keywords:
Fluorescent probe
Ferri ion
PO_4^{3-}
Relay recognition
Cell imaging

ABSTRACT

A novel fluorescent probe XDS based on 4-methylumbelliferone and 2-picolylamine platforms has been designed and synthesized, which behaves fast relay recognition of Fe^{3+} and PO_4^{3-} via a fluorescence "on–off–on" response signal. Probe XDS exhibited very high sensitivity and unique selectivity for Fe^{3+} over other common metal ions, and the detection limit of was 3.2×10^{-7} M. Moreover, the addition of the PO_4^{3-} ions could cause the recovery of fluorescence. This relay recognition feature of probe XDS has potential applications in the determination of trace amount of Fe^{3+} and PO_4^{3-} in environmental systems. Interestingly, fluorescence imaging experiments demonstrated that the probe XDS can also be used to monitoring the intracellular Fe^{3+} in RAMOS cells.

1. Introduction

The design and development of chemosensors for the recognition of cations and anions have attracted noticeable attention due to their important roles in the wide range of environmental, clinical, and biological systems.[1–4] With the comparisons to other instrumental methods such as inductively coupled plasma atomic emission or mass spectroscopy (TCP-AES, ICP-MS), atomic absorption spectroscopy (AAS), electro-chemical methods, etc,[5–11] fluorescent detections have more practical value for sensing and detecting trace amounts ions owing to its favorable superiorities including non-destructive character, high selectivity and sensitivity, fast response and economical method for the detection without any tedious sample pretreatment.[12–14]

Therefore, considerable studies have concentrated on construction of highly efficient and convenient ion probe using spectrophotometric and spectrofluorometric methods.[15,16]

It is well known that iron is one of the most essential trace elements in human body. It is an indispensable ion for most organisms by exhibiting a crucial role in various biological and chemical processes at the cellular level such as oxygen uptake, oxygen metabolism, enzyme catalysis.[17–19] However, its deficiency or excess may lead to hypoferremia or hyperferremia, accordingly. In addition, it has recently been discovered that iron is another key limiting factor for the primary productivity of phytoplankton besides elemental nitrogen, phosphorus and silicon.[20,21] In contrast, phosphates and its derivatives (eg, adenosine triphosphate (ATP)) play a crucial role in signal transduction and energy storage in biological systems.[22,23] Phosphate anions are ubiquitous in biological systems and it plays vital functional roles in cell signaling, membrane integrity, bone mineralization, muscle function and other important biological processes.[24–26] Unfortunately, only a small number of fluorescent anion sensors can effectively distinguish F^-, AcO^-, phosphates and their derivatives.[27–31]

Thus, it is highly desirable to develop a highly selective and sensitive analytical method for the detection of Fe^{3+} and PO_4^{3-} for further study of their physiological and pathophysiological

* Corresponding author.
** Corresponding author.
E-mail addresses: yunwang@ujs.edu.cn (Y. Wang), wlzhang@ujs.edu.cn (W. Zhang).

http://dx.doi.org/10.1016/j.tet.2017.07.018
0040-4020/

functions in living organisms.

Herein, we have prepared a simple and efficient fluorescent probe XDS based on 4-methylumbelliferone and 2-picolylamine platforms for relay recognition of Fe^{3+} and PO_4^{3-}. We chose coumarin as the fluorescent group because of its good fluorescence properties and water solubility. Meanwhile, as a recognition group, 2-aminomethylpyridine can provide the N atoms as excellent coordinating site. Thus, we chose Chloroacetyl chloride as a linker to effectively combine the 4-methylumbelliferone and 2-picolylamine to form a compound XDS with strong fluorescence emission. In this study, we also further investigated in detail the fluorescence performances of the probe XDS. The investigated results demonstrated that the probe XDS exhibits high selectivity, sensitivity and rapid fluorescence response to Fe^{3+} ion over other metal cations in aqueous solution. Moreover, we also explore anion-sensing properties of the in situ-formed [XDS-Fe^{3+}] complexes in the aqueous environment and test trips. As anticipated, the complex exhibited excellent properties for PO_4^{3-} detection according to the strong binding capacity of PO_4^{3-} to Fe^{3+}. At the same time, the performance of XDS for the fluorescence imaging in living cells was also evaluated.

2. Experimental

2.1. Materials and instruments

Unless otherwise noted, all reagents and solvents employed for synthesis were purchased from Aladdin Chemical Reagent Ltd., and used without further purification. All the metal chlorate salts (Al^{3+}, Sr^{2+}, Li^{+}, Cs^{+}, Ca^{2+}, Cd^{2+}, Cr^{3+}, Co^{2+}, Cu^{2+},Fe^{2+}, Fe^{3+},K^{+}, Hg^{2+}, Mg^{2+}, Mn^{2+},Ni^{2+},Na^{+}, Pb^{2+} and Zn^{2+}.) and all anionic sodium salt (PO_4^{3-},F^{-}, Cl^{-}, Br^{-}, I^{-},SO_4^{2-}, SCN^{-}, ClO_4^{-}, CO_3^{2-}, NO_3^{-}, NO_2^{-}, $H_2PO_4^{-}$, HPO_4^{2-}, AcO^{-} and CN^{-}.) were purchased from Sinopharm Chemical Reagent Ltd.,

^1H NMR and ^{13}C NMR spectra were measured using an AVANCE II 400 MHz spectrometer (Bruker, Switzerland). Mass spectra were obtained using a Thermo LXQ Liquid chromatography ion trap mass spectrometer (USA). Fluorescence measurements were taken at a Cary Eclipse fluorescence spectrophotometer (Variance. LTD, Australia). Absorption spectra were recorded with a UV-2450 UV–Vis spectrophotometer (Shimadzu, Japan) at room temperature. Cell experiments were applied on an inverted fluorescence microscope (Leica DMI4000B, Germany).

2.2. Synthesis of XDS

2.2.1. Compound **R**: 2-((4-methyl-2-oxo-2H-chromen-7-yl)oxy) acetyl chloride

Chloroacetyl chloride (0.35 mL) was dissolved in dry CH_2Cl_2 at 0 °C, and then added dropwise to a cooled stirred mixture of 4-MethylμMbelliferone (0.70 g, 4 mmol) and triethylamine (Et_3N) (0.3 mL) in CH_2Cl_2 under N_2 within 1 h, After being stirred over night at room temperature, the reaction mixture was quenched with distilled water and then was extracted three times with 20 mL of CH_2Cl_2. The combined organic layer was dried over anhydrous Na_2SO_4 and removed under reduced pressure to obtain a white solid product. The crude product was purified by recrystallization from ethanol (methanol) to give analytically pure compound **R** (0.93 g) in 93% yield.

2.2.2. Compound XDS: 4-methyl-2-oxo-2H-chromen-7-yl 2-((pyridine-2-ylmethyl) amino)acetate

R (1.006 g, 4 mmol) was dissolved in anhydrous CH_3CN and the solution was added dropwise to a stirred mixture of 2-aminomethylpyridine (0.86 g, 8 mmol), $NaHCO_3$ (0.69 g), K_2CO_3(1.1 g) and KI (1.3 g) at room temperature under N_2 over a period of 30 min and the resulting mixture was stirred for an additional 12 h. Then the resulting mixture was cooled to room temperature, filtered over gravity and the solvent was removed under reduced pressure to afford solid product, which was purified by recrystallization from ethanol to get analytically pure compound XDS (4-methyl-2-oxo-2H-chromen-7-yl 2-((pyridin-2-ylmethyl) amino)acetate) (1.1 g) in 86% yield (Scheme 1). The product is verified by ^1H NMR, ^{13}C NMR, MS (Figs. S1–3). ^1H NMR (400 MHz, DMSO): $\delta = 8.87$ (t, $J = 5.7$ Hz, 1H), 8.51 (d, $J = 4.5$ Hz, 1H), 7.74 (dd, $J = 12.8$, 5.1 Hz, 2H), 7.35–7.21 (m, 2H), 7.09–6.97 (m, 2H), 6.24 (s, 1H), 4.75 (s, 2H), 4.46 (d, $J = 5.9$ Hz, 2H), 2.37 (d, $J = 29.8$ Hz, 3H) ppm; ^{13}C NMR (101 MHz, DMSO): $\delta = 40.62$, 40.41, 40.20, 39.89, 39.75, 39.58, 39.37, 18.61 ppm.

MS: $[M + H]^+$ calcd for $C_{18}H_{16}O_4N_2$: 325.33, found: 325.60.

2.3. Fluorescence spectroscopy

Unless otherwise noted, materials were of analytical grade from commercial suppliers and were used without further purification. Deionized water was used throughout all experiments.

Stock solutions (10 mM) of the various anions of F^{-}, Cl^{-}, Br^{-}, I^{-}, SO_4^{2-}, SCN^{-}, ClO_4^{-}, CO_3^{2-}, NO_3^{-}, $H_2PO_4^{-}$, HPO_4^{2-}, NO_2^{-}, AcO^{-} and CN^{-} in deionized water, were prepared. Stock solutions (10 mM) of various metal ions were prepared from NaCl, CsCl, $PbCl_2$, $CoCl_2$, $ZnCl_2$, $CuCl_2$, $NiCl_2$, $HgCl_2$, $CdCl_2$, $CrCl_3$, $FeCl_2$,$FeCl_3$, LiCl, $MgCl_2$, $CaCl_2$, $AlCl_3$, $SrCl_2$ and $MnCl_2$.

Stock solution of probe XDS (1 mM) was also prepared in deionized water and diluted to prepare the analytical solution (10 μM). For fluorescence measurements, both the excitation and emission slit widths were 5 nm. The excitation wavelength was set at 320 nm.

2.4. Cell culture and imaging studies

The RAMOS cells (Human B lymphocyte tumor cells) were seeded on a 24-well plate and were incubated in medium (supplementing with RPMI 1640, 10% FBS) at 37 °C for 24 h. Subsequently, the cells were incubated with 20 μM of probe XDS at 37° C for 0.5 h and then washing with three times to remove the remaining probe XDS. The cells were then incubated with Fe^{3+}(20 μM) at 37° C for an additional 0.5 h, then 20 μM of PO_4^{3-} were added and incubated for another 0.5 h. The treated cells were rinsed three times with buffered saline. The cell imaging in different stages were obtained by an inverted fluorescence microscope.

2.5. Computational methodology

The density functional theory (DFT) calculations were perused to get the theoretical aspects of the coordinating mode of the probe XDS and Fe^{3+}. The DFT optimizations of probe XDS and XDS-Fe^{3+} complex were carried out using the Gaussian 09 program,[32] in which the B3LYP function was used. The 6-311 + G* and LanL2DZ basis sets were used for the probe XDS and the metal ions, respectively.[33] Besides, the distribution of electronic clouds on both HOMO and LUMO of probe XDS and XDS-Fe^{3+} complex were also studied.

3. Results and discussion

3.1. Fluorescence characterization and selectivity of XDS toward Fe^{3+}

The effect of metal ions on the fluorescence properties of XDS

Please cite this article in press as: Liu R, et al., A fluorescent chemosensor for relay recognition of Fe^{3+} and PO_4^{3-} in aqueous solution and its applications, Tetrahedron (2017), http://dx.doi.org/10.1016/j.tet.2017.07.018

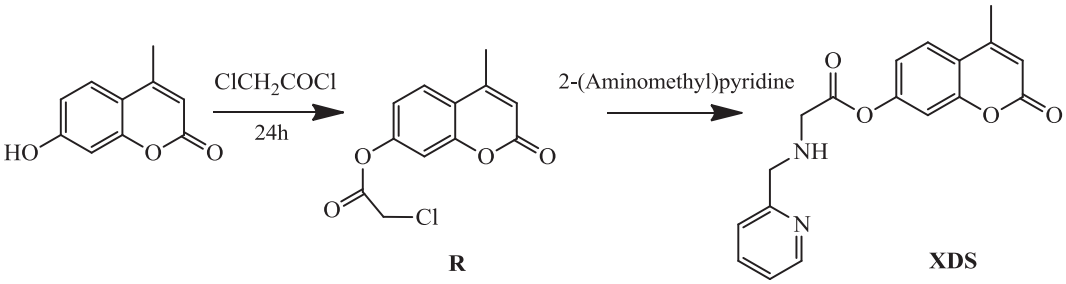

Scheme 1. Synthesis of probe XDS.

was investigated through the naked eye detection in aqueous solution. As shown in Fig. 1, only the mixture of XDS and Fe^{3+} showed a fluorescence quenching phenomenon, the emission color change from blue to colorless can be clearly observed in the presence of Fe^{3+} under UV irradiation (365 nm), while no significant emission color change can be induce by the addition of other metal ions.

Additionally, the response of the probe XDS toward different metal ions was evaluated for affinity toward metal ions through naked eye in the further investigation, another interesting phenomenon was found that the addition of Fe^{3+} not only caused obvious fluorescence change of the probe solution but also a slight color change from colorless to yellow, while no change in color was observed with the addition of other metal ions (Fig. S4).

In the subsequent fluorescence studies, the fluorescence properties of the mixture of XDS and Fe^{3+} were therefore carried out in aqueous solution by fluorescence spectrophotometer. As can be seen from Fig. 2, the free XDS (10 μM) showed a degree of fluorescence intensity with emission maxima around 380 nm, surprisingly, a significant reduction in the fluorescence intensity was observed by the addition of Fe^{3+}, while minor fluorescence changes can be noticed in the presence of other metal ions. The results indicated that XDS can response to Fe^{3+} with high specifity by obvious fluorescence quenching due to the formation of a new complex between XDS and Fe^{3+}.

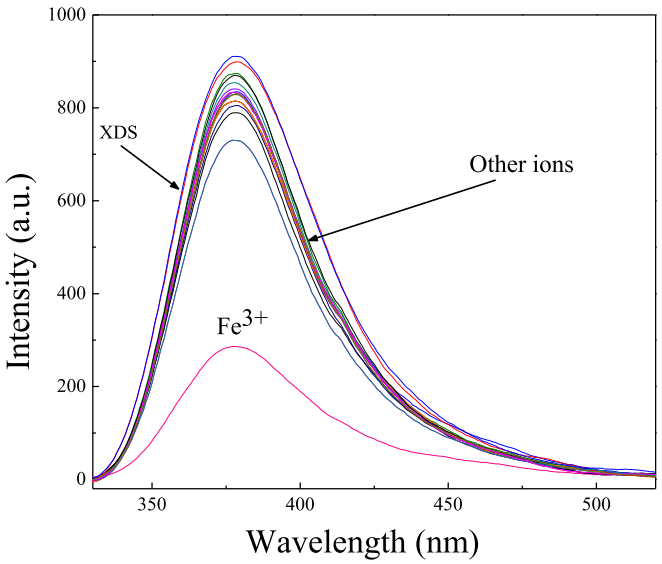

Fig. 2. The fluorescence characterization of XDS and metal ions: the fluorescence response of XDS (10 μM) by mixing with different metal ions (10 equiv.) in aqueous solution.

3.2. The stability of XDS and the respond time on sensing Fe^{3+}

In order to evaluate the stability of XDS and [XDS-Fe^{3+}], first, XDS was irradiated under 365 nm for more than 60 min using the LED source while the fluorescence intensity was investigated by the fluorescence spectrophotometer. Fig. S5 shown that no apparent fluorescence intensity change was observed during this period, which suggested XDS is very stable. Thereafter, once 20 equivalents of Fe^{3+} solution was added to the XDS solution, the fluorescence intensity sharply decreased. The fluorescence signal is then maintained at a steady level for more than 60 min. These results indicated evidently that both of XDS and [XDS-Fe^{3+}] complex are very stable under the test conditions.

The response time is an extremely important factor in characterizing the performance of the fluorescence probe, thus the effect of the respond time on fluorescence intensity of this system was also calculated by an experimental determination of the reaction rate constant in aqueous solution. As shown in Fig. 3a, we concluded that the complexation reaction of XDS and Fe^{3+} belongs to the zero-order reaction. It is generally known that the zero-order reaction rate is independent of the reactant concentration. To provide a complete combination with the probe, we used 10 eq. of Fe^{3+} ions in previous experiments. We also calculated its complete reaction time of about 100 s from its linear equation, less than 2 min. The further experimental results displayed that the fluorescence intensity of XDS was quenched rapidly, reaching a stable value within 2 min after the addition of Fe^{3+} to XDS. This phenomenon proved evidently that the interaction between XDS and

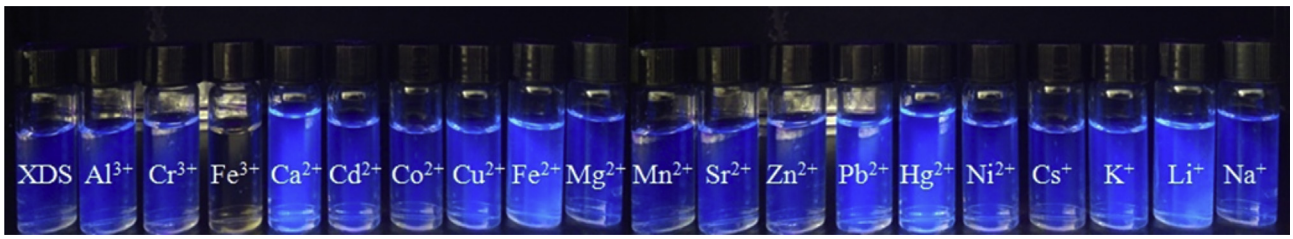

Fig. 1. The luminescence change of the mixture of XDS (20 μM) and various metal ions (10 equiv.) under the UV lamp (λ = 365 nm).

Please cite this article in press as: Liu R, et al., A fluorescent chemosensor for relay recognition of Fe^{3+} and PO_4^{3-} in aqueous solution and its applications, Tetrahedron (2017), http://dx.doi.org/10.1016/j.tet.2017.07.018

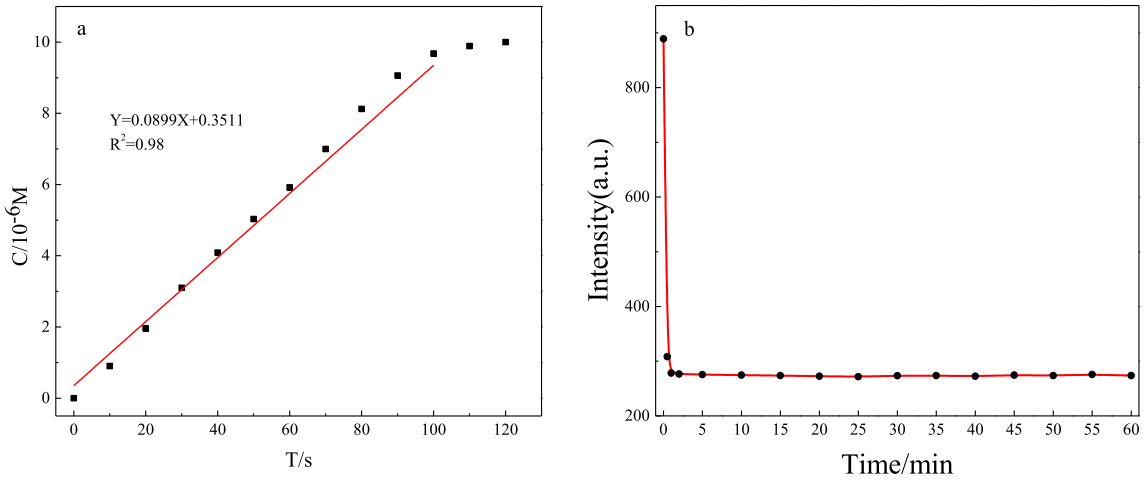

Fig. 3. (a) The determination of the reaction rate constant of the complexation reaction of XDS and Fe^{3+}; (b) Fluorescence quenching profile of addition Fe^{3+} (10 equiv.) to XDS (10 μM) in aqueous solution from 1 to 60 min.

Fe^{3+} can occur directly at room temperature with excellent sensitivity. The rapid, stable complexation provided XDS a potential utility for an on-site rapid detection method for monitoring Fe^{3+} by portable device in field.

3.3. Fluorescence titration

In order to further evaluate the response properties of probe XDS to Fe^{3+}, fluorescence titration experiments with incremental addition of a solution of Fe^{3+} ions were performed. It can be seen from Fig. 4, fluorescence intensity was gradually weakened with the increasing the concentration of Fe^{3+}. As Fig. S6 shown, a good liner relationship (R = 0.989) was noted between (F_0-F) and [Fe^{3+}] at Fe^{3+} concentration from 1 μM to 10 μM. The detection limit was calculated to be 3.2×10^{-7} M (L = 3 σ/K, K = 1.49×10^7, σ = 1.58), much lower than most of the reported in literature. The job's plot revealed 1:1 stoichiometry for the binding between XDS and Fe^{3+} (Fig. 5). The association constant of XDS with Fe^{3+} in aqueous solution was accordingly calculated to be 1.895×10^4 M^{-1} (Fig. S7).

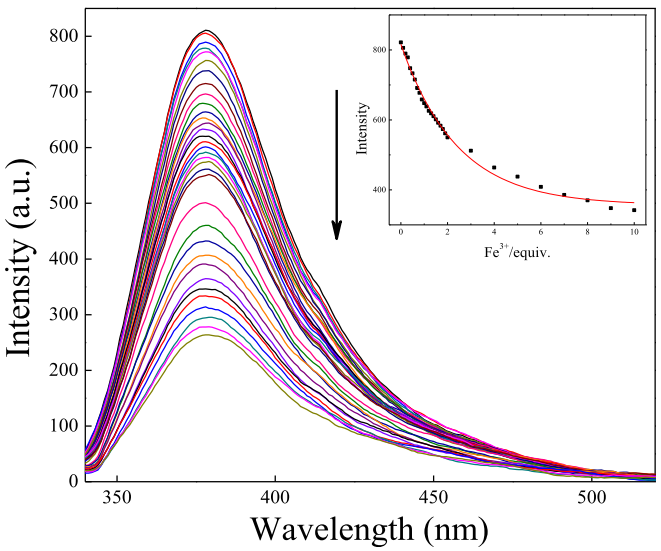

Fig. 4. Fluorescence spectra of probe XDS in 100% aqueous solution upon the addition of Fe^{3+} ions (Ex = 320 nm).

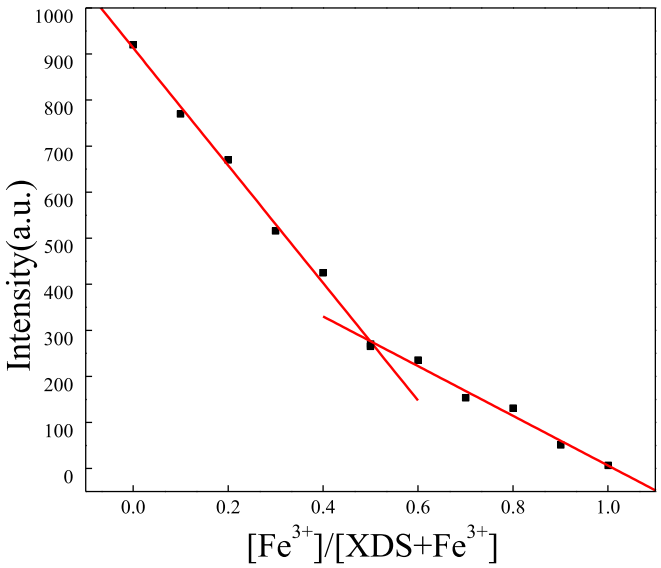

Fig. 5. Job's plot of XDS and Fe^{3+}, which indicated that the stoichiometry of the XDS-Fe^{3+} complex is 1:1.

On the other hand, it must be noted that the probe XDS possessed a large advantage over most reported fluorescent probes. The probe XDS can show the excellent determination for Fe^{3+} in pure water solution, and most of the previously reported fluorescent probes can only be applied in pure organic[36,37] or the organic solvent modified water solution.[34,38–44] The comparisons about the detection limit, linearity range and detection media between the present method and those reported in literature were shown in Table 1.

In addition, in order to check the stability and repeatability of the quantitative determination of Fe^{3+}, we repeated the test for 26 times in 4 days. Our results suggested the established method is very stable for Fe^{3+} determination with RSD of 2.2% (Fig. S8).

3.4. Competition experiments with other metal ions

Selectivity or anti-interference ability is a very important factor in the evaluation of fluorescent probes or sensors. It determines whether the probe or sensor can be performed to an actual sample

Please cite this article in press as: Liu R, et al., A fluorescent chemosensor for relay recognition of Fe^{3+} and PO_4^{3-} in aqueous solution and its applications, Tetrahedron (2017), http://dx.doi.org/10.1016/j.tet.2017.07.018

Table 1
Comparison of the detection limit, detection media and response time for Fe^{3+} between the present method and those reported in literature.

Probes	Detection limit (μM)	Detection media	Response time	References
Rhodamine derivatives	0.396	MeOH/H_2O (1/1)	200 min	34
Rhodamine derivatives	20	CH_3CN/H_2O	30 min	35
Rhodamine derivatives	5	MeOH	–	37
Fluorescent dye	0.469	DMF/H_2O (2/3)	–	38
Rhodamine derivatives	0.105	CH_3OH/H_2O (4/6)	1 min	39
Ratiometric fluorescent	2	DMSO/H_2O (1/99)	–	40
Pyrene derivatives	2.5	CH_3OH/H_2O (6/4)	–	42
Rhodamine derivatives	2.2	MeOH/H_2O (1/9)	–	43
Polypyrrole nanowires	2	EtOH/H_2O	–	44
Rhodamine derivatives	1.5	Aqueous	10 min	45
Silver nanoclusters	0.12	Aqueous	10 min	46
Rhodamine derivatives	0.3	Aqueous	–	47
XDS	0.32	Aqueous	2 min	This study

with a complex matrix. To further investigate the selectivity of XDS to Fe^{3+} against other metal ions, competition experiments were therefore carried out, where the probe was first treated with 10 eq. of various metal ions respectively, including Hg^{2+}, Al^{3+}, Sr^{2+},Cs^{+}, Ca^{2+}, Cd^{2+}, Co^{2+}, Cr^{3+}, Cu^{2+}, Fe^{2+}, Li^{+}, K^{+}, Mg^{2+}, Mn^{2+}, Ni^{2+}, Pb^{2+}, Na^{+} and Zn^{2+}, followed by adding 10 eq. of Fe^{3+} ions. As shown in Fig. 2, the fluorescence intensities of these mixtures were almost as same as that of free XDS solution with the minor significant change. However, a noticeable fluorescence quenching has occurred obviously with the addition of Fe^{3+} into the above mixed solutions of XDS and the competitive metal ions (Fig. 6a).

Meanwhile, in order to check the ability of using XDS as a practical ion selective fluorescent chemosensor for Fe^{3+} in real complicated samples, we also investigated the interference of mixed 18-reference metal ions on the interaction between XDS and Fe^{3+}. In this experiment, XDS aqueous solution (10 μM) was treated with 10 eq. of 18 reference metal ions, the concentration of each metal ion was 100 μM. As expected, the fluorescence of XDS solution with the presence of the mixture of 18 metal ions showed almost no obvious change (Fig. 6b, yellow line). In contrast, the fluorescence reduced greatly when Fe^{3+} solution was added into the above mixture (Fig. 6b, red line), which revealed that Fe^{3+} displays an effective fluorescence quenching effect to XDS. From these distinct observations, it is confirmed that XDS can be used as a practical ion selective fluorescent probe for Fe^{3+} detection in the presence of most competing metal ions.

3.5. Effect of pH

In addition, in order to explore the effect of pH value on the fluorescence of XDS and [XDS-Fe^{3+}], we also carried out those experiments in a series of solutions with pH ranging from pH 2 to 12 maintained by the respective buffers.

The results are shown in Fig. 7, as can be seen that the emission behavior of sensor XDS almost remained constant in the pH range 4.0–7.0. However, the fluorescence intensity of the sensor decreased and slightly increased when the pH value of solution is below 4.0 and above 8.0 due to protonation and deprotonation of urea –NH function, respectively. Similarly, upon the addition of Fe^{3+} (10 equiv.), the fluorescence intensity was slightly increased by the pH value in pH > 8 solution (Fig. 7 red spot). This is possibly attributed to the hydrolysis reaction of Fe^{3+} when pH value is above 9. Thus, the investigated results demonstrated that sensor XDS is suitable for the detection of Fe^{3+} in the pH range from 4.0 to 7.0.

3.6. Competition experiments with common anions

Considering practical application, we have not only discussed the interference of common metal ions on the detection of XDS towards Fe^{3+}, but also investigated the fluorescence signal response of probe XDS toward Fe^{3+} in the presence of various coexistent anions such as F^-, Cl^-, Br^-, I^-, SO_4^{2-}, SCN^-, ClO_4^-, PO_4^{3-}, $H_2PO_4^-$, HPO_4^{2-}, CO_3^{2-}, NO_3^-, NO^{2-}, AcO^- and CN^-. Interestingly, a remarkable fluorescence recovery from colorless to blue can be clearly noted with the addition of 10 equiv. of PO_4^{3-} to the [XDS-Fe^{3+}] complex. At the same time, a minor fluorescence recovery of the XDS-Fe^{3+} complex system can be noticed with the addition of $H_2PO_4^-$. However, its effect on the fluorescence recovery of the XDS-Fe^{3+} complex system is minimal compared to PO_4^{3-}(Fig. 8).

As Fig. 9a shown, an intense fluorescence emission at 378 nm

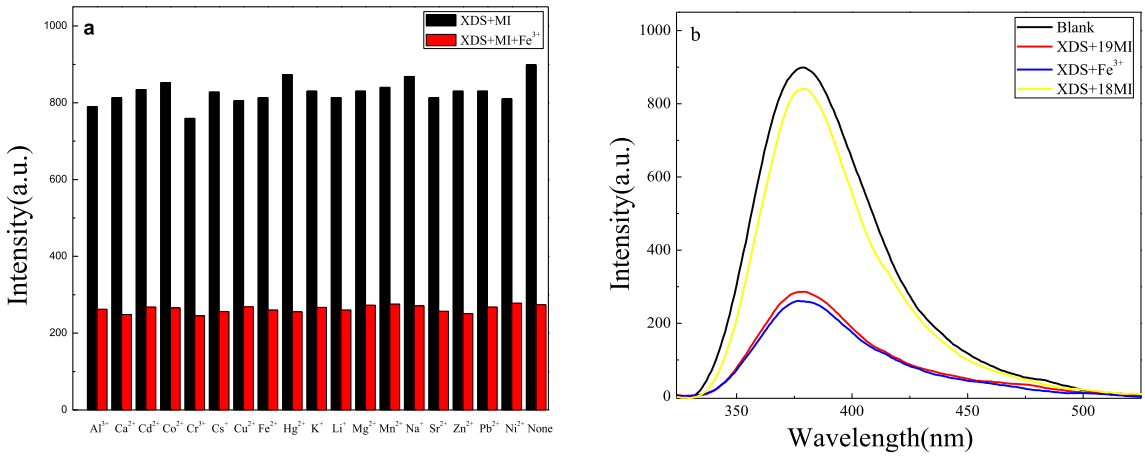

Fig. 6. Fluorescence intensity for probe XDS (10 μM) with Fe^{3+} in the presence of single competitive metal ions (a); Fluorescence intensity for probe XDS (10 μM) with Fe^{3+} in the presence of mixed competitive metal ions (b); Ex = 320 nm.

Please cite this article in press as: Liu R, et al., A fluorescent chemosensor for relay recognition of Fe^{3+} and PO_4^{3-} in aqueous solution and its applications, Tetrahedron (2017), http://dx.doi.org/10.1016/j.tet.2017.07.018

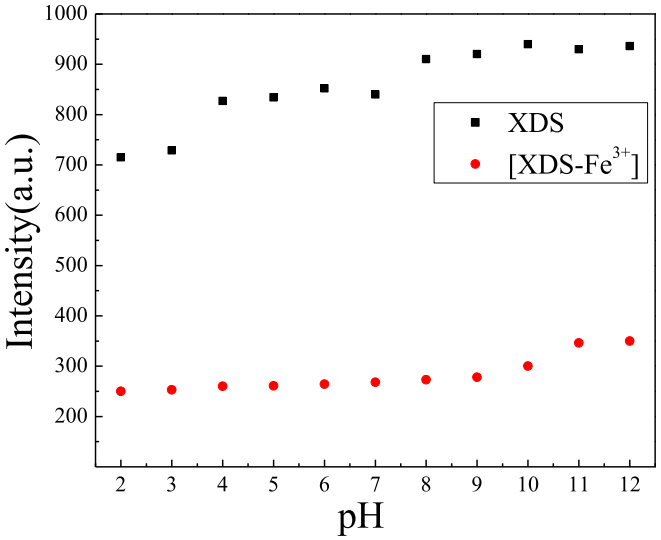

Fig. 7. The influence of pH value of solution on the fluorescence of XDS and [XDS-Fe^{3+}].

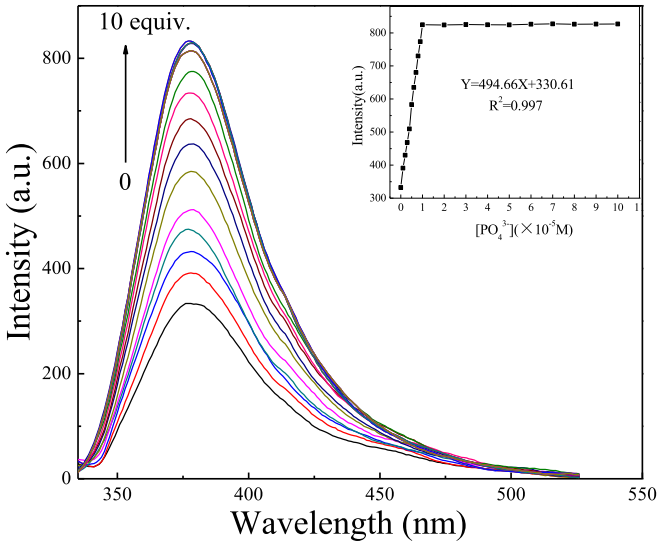

Fig. 10. Fluorescence spectra of [XDS-Fe^{3+}] complex (10 μM) upon the progressive addition of PO_4^{3-} in various concentration ranges.

was observed when excited at 320 nm with the addition of PO_4^{3-} and a weak fluorescence emission recovery of the XDS-Fe^{3+} complex system can be noticed with the addition of $H_2PO_4^-$. In contrast, no significant response was observed when the [XDS-Fe^{3+}] complex was mixed with 10 equiv. of the other various anions of F^-, Cl^-, Br^-, I^-,SO_4^{2-}, SCN^-, ClO_4^-, CO_3^{2-}, NO_3^-, NO^{2-}, HPO_4^{2-}, AcO^- and CN^- respectively. The selective recognition of [XDS-Fe^{3+}] complex towards PO_4^{3-} was hardly affected by these commonly coexistent anions (Fig. 9b). These experimental results indicated that the [XDS-Fe^{3+}] complex can function as a fluorescent probe for PO_4^{3-} via a fluorescence "turn-on" mechanism.

The fluorescence titrations of PO_4^{3-} were also conducted using a 10 μM solution of [XDS-Fe^{3+}] complex (10 μM + 10 μM) in aqueous solution upon progressive addition of PO_4^{3-} in various concentration ranges to the solution. An obvious increase in the fluorescence intensity at 378 nm was observed when excited at 320 nm (Fig. 10). Further increase in the concentration of PO_4^{3-} (>10 μM) led to no further fluorescence increase (Fig. 10, inset), which clearly

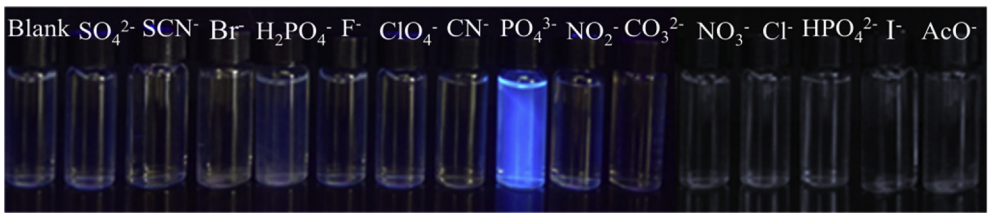

Fig. 8. The luminescence change of the mixture of [XDS-Fe^{3+}] (10 μM) and various anions (10 equiv.) under the UV lamp (λ = 365 nm).

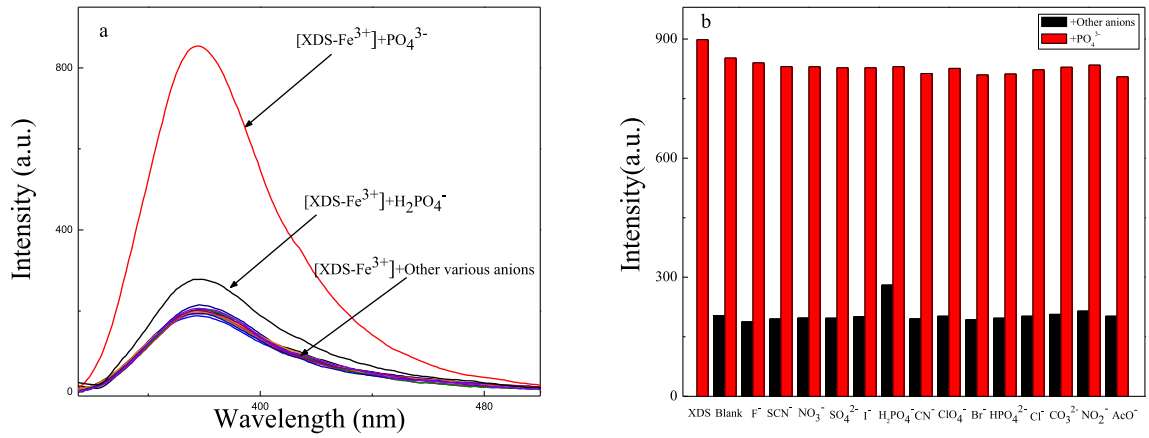

Fig. 9. (a) The fluorescence spectra changes of [XDS-Fe^{3+}] complex system (10 μM XDS + 10 equiv. Fe^{3+}) in the presence of various anions (F^-, Cl^-, Br^-, I^-, AcO^-, SO_4^{2-}, $H_2PO_4^-$, HPO_4^{2-}, CO_3^{2-}, ClO_4^-, SCN^-, NO_3^-, NO_2^- and CN^- (10 equiv., respectively)) in aqueous solutions; (b) the influence of single anions to the interaction between [XDS-Fe^{3+}] and PO_4^{3-}, (Ex = 320 nm).

Please cite this article in press as: Liu R, et al., A fluorescent chemosensor for relay recognition of Fe^{3+} and PO_4^{3-} in aqueous solution and its applications, Tetrahedron (2017), http://dx.doi.org/10.1016/j.tet.2017.07.018

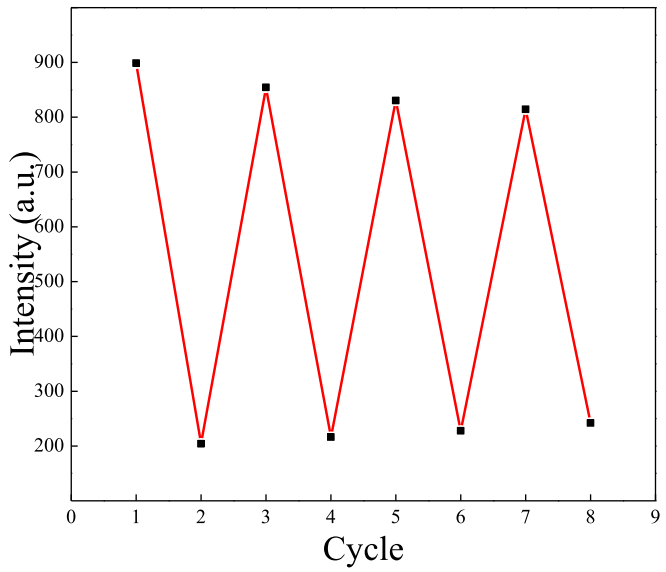

Fig. 11. Reversible switching cycles of fluorescence intensity by alternate addition of Fe^{3+} and PO_4^{3-} ions.

demonstrated a 1:1 stoichiometry between the [XDS-Fe^{3+}] complex and PO_4^{3-}.Based on the fluorescence titration data (Fig. 10), we calculated the detection limit is 8.0×10^{-7} M.

It is also noteworthy that PO_4^{3-} induced emission characteristics, which are almost identical to XDS in the absence of any guest species, suggest that the observed fluorescence response should be derived from the regeneration of the acceptor XDS, possibly due to a reduction of Fe^{3+} to $FePO_4$ to regenerate the XDS. It is generally known that the $FePO_4$ ($Ksp = 1.3 \times 10^{-22}$) is indissoluble in aqueous solutions.[48] In the further investigations, we also found that the addition of PO_4^{3-} could induce the flocculent precipitation in the high concentration experiments, the results are shown in Fig. S9. The addition of PO_4^{3-} could also cause the fluorescence recovery of [XDS-Fe^{3+}] complex system, and the fluorescence of the system could quench again with the addition of Fe^{3+} ions. These phenomena further confirmed that the binding capacity of PO_4^{3-} to Fe^{3+} is stronger than that of the probe XDS. Thus, it is reasonable to surmise that the bound Fe^{3+} in [XDS-Fe^{3+}] complex can be separated by PO_4^{3-}. The orthophosphate (PO_4^{3-}) anion can induce the precipitation of ferric ion with the regeneration of the probe XDS.

As shown in Fig. 11, the addition of 10 equiv of PO_4^{3-} to the solution containing XDS (10 μM) and Fe^{3+} (10 equiv.) immediately restored the emission to the original level of XDS. The alternate additions of Fe^{3+} and PO_4^{3-} to the probe XDS solution caused the obvious changes in the fluorescence intensity. This “on-off-on” switching process could be repeated several times with little fluorescent efficiency loss.

Upon the addition of PO_4^{3-}, the recovery of fluorescence was observed with short response time. These results clearly revealed that XDS-Fe^{3+} can serve as a relay probe to detect phosphate (PO_4^{3-}) anion with high selectivity and sensitivity in pure water.

3.7. Quantum mechanical calculations

The optimized structures of probe XDS and XDS-Fe^{3+} complex were shown in Fig. 12, The results showed that metal ions and probe XDS are combined with a ratio of 1:1 and the Fe^{3+} ion was chelated through three coordination sites, which is pyridine nitrogen, amino nitrogen and oxygen atoms of coumarin and the bond length are 1.96161 Å, 1.75464 Å, and 2.07515 Å. The UV spectrum of XDS-Fe^{3+} complex has also been made by time-dependent density functional method (TD-DFT). The solvation model is Polarizable Continuum Model (PCM) and water as the solvent. As shown in Fig. 13, the theory maximum absorption

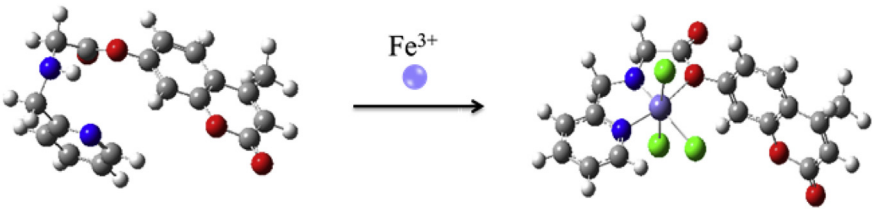

Fig. 12. The optimized geometry of XDS and the XDS-Fe^{3+} complex at the B3LYP level of theory (the green atoms is chlorine).

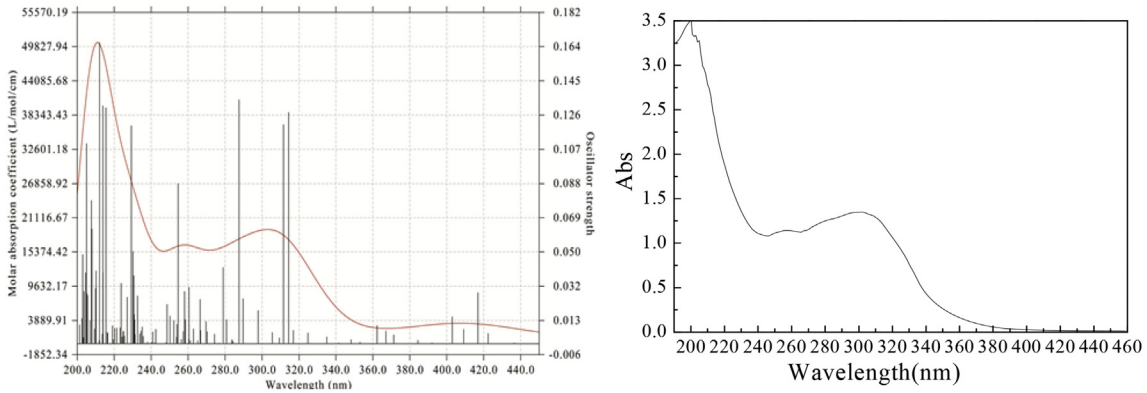

Fig. 13. (a) The UV–Vis spectra of XDS-Fe^{3+} complex at the B3LYP/LanL2DZ level of theory; (b) the UV–Vis spectra of XDS-Fe^{3+} complex in aqueous solution, the corresponding molar extinction coefficient (ε = A/bc) is 3.33×10^4 L mol^{-1} cm^{-1}.

Please cite this article in press as: Liu R, et al., A fluorescent chemosensor for relay recognition of Fe^{3+} and PO_4^{3-} in aqueous solution and its applications, Tetrahedron (2017), http://dx.doi.org/10.1016/j.tet.2017.07.018

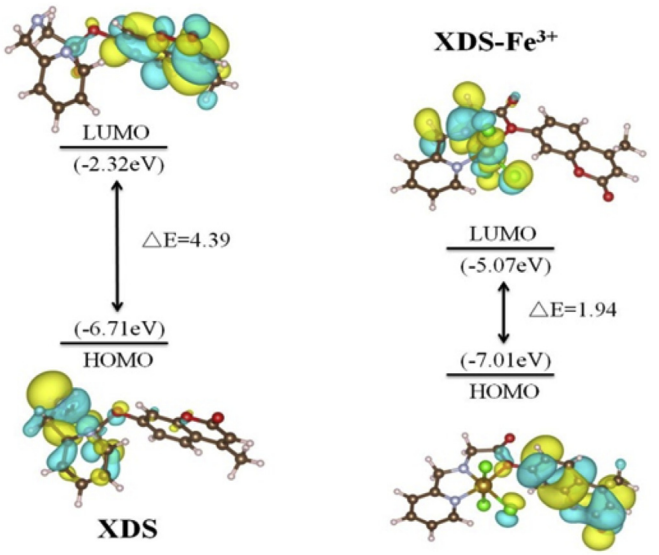

Fig. 14. Molecular orbitals plots of HOMO and LUMO of free XDS and XDS-Fe^{3+} complex, and the orbital plots is generated by the VESTA software.[50]

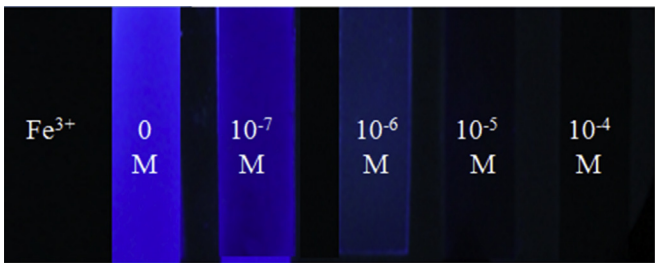

Fig. 15. Photographs of the test strips with XDS (10^{-5} mol/L) for the detection of Fe^{3+} in the aqueous solution with different concentrations.

Fig. 16. Photographs of the test strips with [XDS-Fe^{3+}] (10 μM) for the detection of PO_4^{3-} in aqueous solution. (A–C): XDS, XDS + Fe^{3+}, [XDS-Fe^{3+}] + PO_4^{3-}.

wavelength (λ_{max}) is 305 nm. There is a negligible error to the experimental value (λ_{max} = 308 nm). The UV–vis absorption spectrum obtained by theoretical calculations is indeed strikingly similar to the experimentally measured spectra, which is beyond our expectation.

The frontier molecular orbital and energy level of the free XDS and the XDS-Fe^{3+} complex were shown in Fig. 14. For free XDS, the localized charge density of HOMO of free XDS localized on the pyridine group end and the LUMO is localized on the coumarin group. There is an obvious intramolecular charge transfer and the fluorescence being emitted from the coumarin group, consistent with our experimental observations. But the molecular orbital structure of XDS-Fe^{3+} complex is distinctly different from that of XDS. The charge density of the HOMO of XDS-Fe^{3+} complex is localized on coumarin group and the LUMO is mainly localized on the metal ions and nearby groups. The introduction of Fe^{3+} ions has destroyed the original charge transfer mode. The change of electronic structure led to the change of optical properties. In addition, the paramagnetic and unfilled d-orbital of the Fe^{3+} ions are other reasons for fluorescence quenching.[49]

3.8. Determinations in test strips

To investigate the practical application of probe XDS, test strips were prepared by immersing a silica gel plate into solutions of XDS (10 μM), and then drying in air. The test strips containing probe XDS were used to sense iron ions. For the iron ion solution, different test strips were immersed for 10 s, and then a noticeable emission color change was observed under UV lamp (365 nm). As the iron ion concentration increased, the fluorescence quenched gradually (Fig. 15). However, an apparent fluorescence recovery from colorless to blue can be noticed immediately when these test strips were immersed into 10 μM of PO_4^{3-}(Fig. 16). These results demonstrated a convenient application of XDS for the relay recognition of Fe^{3+} and PO_4^{3-}.

3.9. Fluorescence imaging in RAMOS cells

In order to examine the ability of XDS to track the level of intracellular Fe^{3+} and PO_4^{3-}, RAMOS cells were used for this experiment. Firstly, the cells were incubated with probe XDS (20 μM) for 30 min at 37 °C and then washed 3 times to remove excess probe XDS. The Fig. 17a and b showed bright-field and fluorescence images of RAMOS cells after treatment with XDS. The cells loaded with XDS showed obvious fluorescence. 20 μM of Fe^{3+} were supplemented to the cells and the cells were incubated at 37 °C for another 30 min. The fluorescence from the intracellular almost complete disappearance of fluorescence was observed in Fig. 17c. Obvious changes of fluorescence indicated that probe XDS is cell membrane permeable and capable of imaging of Fe^{3+} in the living cells. The cells then were incubated with PO_4^{3-}(20 μM) for another 30 min. The cells showed fluorescence recovered after the addition of PO_4^{3-}(Fig. 17d). The results suggested that the XDS can be used for the detection of the level of intracellular Fe^{3+} and PO_4^{3-}.

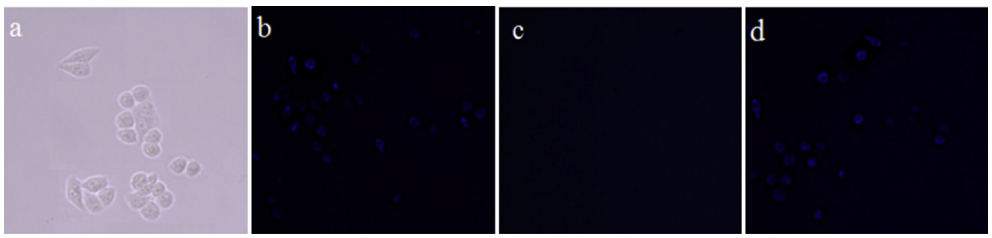

Fig. 17. Fluorescence images of probe XDS in RAMOS cells: bright-field images (a) and fluorescence images of RAMOS cells incubat with probe XDS (b), 20 μM of Fe^{3+} (c), 20 μM of Fe^{3+} and 20 μM of PO_4^{3-} (d), respectively.

Please cite this article in press as: Liu R, et al., A fluorescent chemosensor for relay recognition of Fe^{3+} and PO_4^{3-} in aqueous solution and its applications, Tetrahedron (2017), http://dx.doi.org/10.1016/j.tet.2017.07.018

4. Conclusion

In conclusion, we have designed and synthesized a novel fluorescent probe XDS based on 4-methylumbelliferone and 2-picolylamine platforms. It displayed high selectivity and sensitivity for Fe^{3+} in 100% aqueous solution with a significant fluorescence quenching effect to form [XDS-Fe^{3+}] complex. The addition of PO_4^{3-} could cause the recovery of fluorescence. So the [XDS-Fe^{3+}] complex could relay recognize the PO_4^{3-}. This "on-off-on" switching process could be repeated at several times and the detection of Fe^{3+} and PO_4^{3-} was not disrupted by the presence of other competing ions. The low detection limit (0.32 μM) makes it possible to detect trace amounts of iron ions. Also, probe XDS was successfully applied in fluorescence imaging of living cells.

Acknowledgements

This work was supported by the National Natural Science Foundation of China (Nos. 31470434, 21576124, 21507047 and 21676124), China Postdoctoral Science Foundation funded project (No. 2017M610308), Zhenjiang Social development project (No. SH2016019), and the Project supported by the Science Foundation of Jiangsu Entry-exit Inspection Quarantine Bureau (Nos. 2016KJ51 and 2017KJ47).

Appendix A. Supplementary data

Supplementary data related to this article can be found at http://dx.doi.org/10.1016/j.tet.2017.07.018.

References

1. Cort AD, Forte G, Schiaffino L. Anion recognition in water with use of a neutral uranyl-salophen receptor. *J Org Chem*. 2011;76:7569–7572.
2. Li YP, Yang HR, Zhao Q, Song WC, Han J, Bu XH. Ratiometric and selective fluorescent sensor for Zn^{2+} as an "off-on-off" switch and logic gate. *Inorg Chem*. 2012;51:9642–9648.
3. Zhao L, Ren P, Zhang Z, Fang M, Shi W, Cheng P. Synthesis, crystal structures and fluorescence properties of four mixed-ligands Zn(II) and Cd(II) coordination compounds. *Sci China Ser B*. 2009;52:1479–1484.
4. Yang Y, Wang Y, Peng Y. A bifunctional, colorimetric and fluorescent probe for recognition of Cu^{2+} and Hg^{2+} and its application in molecular logic gate. *Sci China Chem*. 2013;57:289–295.
5. Nomngongo PN, Ngila JC. Determination of trace Cd, Cu, Fe, Pb and Zn in diesel and gasoline by inductively coupled plasma mass spectrometry after sample clean up with hollow fiber solid phase microextraction system. *Spectrochim Acta B*. 2014;98:54–59.
6. Caldas LF, Brum DM, de Paula CE, Cassella RJ. Application of the extraction induced by emulsion breaking for the determination of Cu, Fe and Mn in used lubricating oils by flame atomic absorption spectrometry. *Talanta*. 2013;110:21–27.
7. Shervedani RK, Hatefi-Mehrjardi A, Asadi-Farsani A, Shervedani RK, Hatefi-Mehrjardi A, Asadi-Farsani A. Sensitive determination of iron(III) by gold electrode modified with 2-mercaptosuccinic acid self-assembled monolayer. *Anal Chim Acta*. 2007;601:164–171.
8. Hosseini MS, Raissi H, Madarshahian S. Synthesis and application of a new chelating resin functionalized with 2, 3-dihydroxy benzoic acid for Fe(III) determination in water samples by flame atomic absorption spectrometry. *React Funct Polym*. 2006;66:1539–1545.
9. Weber G, Neumann G, Römheld V. Speciation of iron coordinated by phytosiderophores by use of HPLC with pulsed amperometric detection and AAS. Analytical and Bioanalytical Chemistry. *Anal Bioanal Chem*. 2002;373:767–771.
10. Huang C, Hu B. Silica-coated magnetic nanoparticles modified with g-mercaptopropyltrimethoxysilane for fast and selective solid phase extraction of trace amounts of Cd, Cu, Hg, and Pb in environmental and biological samples prior to their determination by inductively coupled plasma mass spectrometry. *Spectrochim Acta A*. 2008;63:437–444.
11. Zamani HA, Faridbod F. Liquid membrane potentiometric sensor for determination of Fe^{3+} ion. *J Anal Chem*. 2014;69:1073–1078.
12. Liu Z, He W, Guo Z. Metal coordination in photoluminescent sensing. *Chem Soc Rev*. 2013;42:1568–1600.
13. Silva AP, Gunaratne HQ, Gunnlaugsson T, et al. Signaling recognition events with fluorescent sensors and switches. *Chem Rev*. 1997;97:1515–1566.
14. Hu ZQ, Feng YC, Huang HQ, et al. Fe^{3+}-selective fluorescent probe based on Rhodamine B and its application in bioimaging. *Sens Actuat B Chem*. 2011;156:428–432.
15. Legin AV, Kirsanov DO, Babain VA, Borovoy AV, Herbst RS. Cross-sensitive rare-earth metal sensors based on bidentate neutral organophosphorus compounds and chlorinated cobalt dicarbollide. *Anal Chim Acta*. 2006;572:243–247.
16. Kirsanov DO, Legin AV, Babain VA. Polymeric sensors based on extraction systems for determination of rare-earth metals. *Russ J Appl Chem*. 2005;78:568–573.
17. Crabtree RH. Metal ions at work. *Science*. 1994;266:1591–1592.
18. Cairo G, Pietrangelo A. Iron regulatory proteins in pathobiology. *Biochem J*. 2000;352:241–250.
19. Eisenstein RS. Iron regulatory proteins and the molecular control of mammalian iron metabolism. *Annu Rev Nutr*. 2000;20:627–662.
20. Geider RJ. Biological oceanography—complex lessons of iron uptake. *Nature*. 1999;400:815–816.
21. Tyrrell T. The relative influences of nitrogen and phosphorus on oceanic primary production. *Nature*. 1999;400:525–531.
22. Gaidamauskas E, Parker H, Kashemirov BA, et al. Complexation of bisphosphonates with ytterbium(III): application of phosphate and ATP detection assay based on Yb^{3+}-pyrocatechol violet. *J Inorg Biochem*. 2009;103:1652–1657.
23. Shervedani RK, Pourbeyram S. Zirconium immobilized on gold-mercaptopropionic acid self-assembled monolayer for trace determination of phosphate in blood serum by using CV, EIS, and OSWV. *Biosens Bioelectron*. 2009;24:2199–2204.
24. Chen CC, Chen YZ, Huang YJ, Sheu JT. Using silicon nanowire devices to detect adenosine triphosphate liberated from electrically stimulated HeLa cells. *Biosens Bioelectron*. 2011;26:2323–2328.
25. Gaidamauskas E, Saejueng K, Holder AA, et al. Metal complexation chemistry used for phosphate and nucleotide determination: an investigation of the Yb^{3+}-pyrocatechol violet sensor. *J Biol Inorg Chem*. 2008;13:1291–1299.
26. Samanta A, Vendrell M, Das R, Chang YT. Development of photostable near-infrared cyanine dyes. *Chem Commun*. 2010;46:7406–7408.
27. Song KC, Kim H, Kang ML, Lee YS, Do YK, Lee MH. Ratiometric fluorescence sensing of fluoride ions by triarylborane-phenanthroimidazole conjugates. *Sens Actuat B Chem*. 2013;176:850–857.
28. Kim SK, Seo D, Han SJ, et al. A new imidazolium acridine derivative as fluorescent chemosensor for pyrophosphate and dihydrogen phosphate. *Tetrahedron*. 2008;64:6402–6405.
29. Kondo S, Takai R. Selective detection of dihydrogen phosphate anion by fluorescence change with tetraamide-based receptors bearing isoquinolyl and quinolyl moieties. *Org Lett*. 2013;15:538–541.
30. Cao X, Lin W, Yu Q, Wang J. Ratiometric sensing of fluoride anions based on a BODIPY-coumarin platform. *Org Lett*. 2015;13:6098–6101.
31. Jadhav JR, Ahmad MW, Kim HS. Selective recognition of $H_2PO_4^-$ by a cholestane-imidazole-zinc ensemble. *Tetrahedron Lett*. 2012;53:2627–2631.
32. Frisch MJ, Trucks GW, Schlegel HB, et al. Gaussian, Inc. Wallingford CT. 2013.
33. Tang X, Han J, Wang Y, et al. A fluorescent chemosensor for Cu^{2+} ions and its application in cell imaging. *Tetrahedron*. 2017;73:1367–1373.
34. Bao XF, Cao XW, Nie XM, et al. A new selective fluorescent chemical sensor for Fe^{3+} based on rhodamine B and a 1,4,7,10-tetraoxa-13-azacyclopentadecane conjugate and its imaging in living cells. *Sens Actuat B Chem*. 2015;208:54–66.
35. Chai MM, Zhang D, Wang M, Hong HJ, Ye Y, Zhao YF. Four Rhodamine B-based fluorescent chemosensor for Fe^{3+} in aqueous solution. *Sens Actuat B Chem*. 2012;174:231–236.
36. Li P, Zhao Y, Yao L, Nie HR, Zhang M. A simple, selective, fluorescent iron(III) sensing material based on peripheral carbazole. *Sens Actuat B Chem*. 2014;191:332–336.
37. She MY, Yang Z, Yin B, et al. A novel rhodamine-based fluorescent and colorimetric "off-on" chemosensor and investigation of the recognizing behavior towards Fe^{3+}. *Dyes Pigments*. 2012;92:1337–1343.
38. Yang L, Yang W, Xu DM, Zhang ZY, Liu AF. A highly selective and sensitive Fe^{3+} fluorescent sensor by assembling three 1,8-naphthalimide fluorophores with a tris(aminoethylamine) ligand. *Dyes Pigments*. 2013;97:168–174.
39. Wang CC, Zhang D, Huang XY, et al. A fluorescence ratiometric chemosensor for Fe^{3+} based on TBET and its application in living cells. *Talanta*. 2014;128:69–74.
40. Wang M, Wang JG, Xue WJ, Wu AX. A benzimidazole-based ratiometric fluorescent sensor for Cr^{3+} and Fe^{3+} in aqueous solution. *Dyes Pigments*. 2013;97:475–480.
41. Casanueva Marenco MJ, Fowley C, Hyland BW, Galindo-Riano D, Sahoo SK, Callan JF. A new fluorescent sensor for the determination of Iron(III) in semi-aqueous solution. *J Fluoresc*. 2012;22:795–798.
42. Fegade U, Tayade S, Chaitanya GK, Attarde S, Kuwar A. Fluorescent and chromogenic receptor bearing amine and hydroxyl functionality for iron(III) detection in aqueous solution. *J Fluoresc*. 2014;24:675–681.
43. Liu SR, Wu SP. New aqueous-soluble highly selective fluorescent chemosensor for Fe(III) ions and its application to living cell imaging. *Sens Actuat B Chem*. 2012;171–172:1110–1116.
44. Wang ML, Meng GW, Huang Q, Xu QL, Liu GD. A GBI@PPyNWs-based prototype of reusable fluorescence sensor for the detection of Fe^{3+} in aqueous solution. *Anal Methods*. 2012;4:2653–2656.
45. Wang JH, Zhang D, Liu YQ, et al. A N-stabilization rhodamine-based fluorescent chemosensor for Fe^{3+} in aqueous solution and its application in bioimaging. *Sens Actuat B Chem*. 2014;191:344–350.
46. Chen Z, Lu DT, Zhang GM, Yang J, Dong C, Shuang SM. Glutathione capped silver nanoclusters-based fluorescent probe for highly sensitive detection of Fe^{3+}. *Sens Actuat B Chem*. 2014;202:631–637.

Please cite this article in press as: Liu R, et al., A fluorescent chemosensor for relay recognition of Fe^{3+} and PO_4^{3-} in aqueous solution and its applications, Tetrahedron (2017), http://dx.doi.org/10.1016/j.tet.2017.07.018

47. Du YY, Chen M, Zhang YX, et al. Determination of iron(III) based on the fluorescence quenching of rhodamine B derivative. *Talanta*. 2013;106:261–265.
48. Scaccia S, Carewska M, Bartolomeo AD, Prosini PP. Thermoanalytical investigation of iron phosphate obtained by spontaneous precipitation from aqueous solutions. *Thermochim Acta*. 2002;383:145–152.
49. Li ZX, Zhang LF, Zhao WY, Li XY, Guo YK. Fluoranthene-based pyridine as fluorescent chemosensor for Fe^{3+}. *Inorg Chem Commun*. 2011;14:1656–1658.
50. Momma K, Izumi F. VESTA 3 for three-dimensional visualization of crystal, volumetric and morphology data. *J Appl Crystallogr*. 2011;44:1272–1276.

Please cite this article in press as: Liu R, et al., A fluorescent chemosensor for relay recognition of Fe^{3+} and PO_4^{3-} in aqueous solution and its applications, Tetrahedron (2017), http://dx.doi.org/10.1016/j.tet.2017.07.018